PHILOSOPHICAL TRANSACTIONS OF THE ROYAL SOCIETY A MATHEMATICAL, PHYSICAL & ENGINEERING SCIENCES

The Radioemission from Flares: Impulsive Phase and Type III Bursts

Monique Pick

Phil. Trans. R. Soc. Lond. A 1980 **297**, 587-593
doi: 10.1098/rsta.1980.0234

Phil. Trans. R. Soc. Lond. A **297**, 587–593 (1980) [587]
Printed in Great Britain

The radioemission from flares: impulsive phase and type III bursts

By Monique Pick
Meudon Observatory, 92190 *Meudon*, *France*

During solar flares, two distinct phases of acceleration can be distinguished. The first is an impulsive phase which does not last more than a fraction of a minute and which consists of the acceleration of electrons of about 100 keV. During the second phase, the particles reach higher energies (more than 1 MeV for electrons) and the development is more gradual. This paper mainly concerns the impulsive phase. Recent microwave and X-ray observations are reviewed. Both emissions result from the same electron distribution. Two principal models exist in the literature: the non-thermal model and the 'quasi-thermal' model. They differ in the particle distribution.

During the impulsive phase, type III radiobursts are observed. Their generation is due to energetic electrons streaming outward through the corona and the interplanetary medium. The mechanism of radiation is briefly reviewed. Recent *in situ* measurements by space experiments and radio observations are shown. Some coronal type III burst observations at metre and decametre wavelengths are reviewed. Conclusions concerning in particular the electron beam characteristics are suggested.

It is now proved beyond doubt that particles are accelerated in two distinct phases during a flare. This was suggested more than 20 years ago by microwave observations of radiobursts (see review by Kundu 1965). Later on, these two phases were clearly identified with X-ray observations which supplied the spectrum of electron energies.

During the first phase, the fast electrons (10–100 keV) produce in the low corona an *impulsive* X-ray and microwave burst, and simultaneously a so-called type III radioburst is often detected which is produced higher in the corona. The impulsive burst does not last for more than a fraction of a minute. During the second phase, the accelerated electrons correspond to a different spectrum and reach energies greater than during the first phase (more than 1 MeV) (Frost & Dennis 1971) (see figure 1). The corresponding X-ray burst exhibits a more gradual development and can exceed many minutes. The particle acceleration is probably related to the production of the shock wave in the corona. Several kinds of radioburst are produced in association with this second phase.

The impulsive phase: microwave and hard X-ray emissions

The hard X-ray emission consists of one or several peaks with a duration of a few seconds, as shown by the ESRO TD-1A satellite experiment (figure 2) (Hoyng *et al.* 1976).

Because of the similarity in the time variation of the X-ray and microwave radiations, it is believed that both emissions result from the same electron distribution. The usual model assumes that the microwave burst is due to gyrosynchrotron emission by moderately relativistic electrons and that the X-ray burst is attributed to electron Bremsstrahlung on a thick cold target. In this model, the electron distribution is characterized by a *non-thermal tail* (Kane 1974) and a large number of fast electrons is required, typically 10^{34} to 10^{37} electrons s^{-1} with an energy greater than 25 keV for a power law distribution corresponding to an index γ from 3 to 5 (table 1).

A more recent approach (Ramaty *et al.* 1978; Smith *et al.* 1978; Dulk *et al.* 1978) assumes that the electrons are heated in bulk and correspond to a Maxwellian energy distribution (table 1). In contrast to the non-thermal model, the existence of a high-energy tail is not required. The gyrosynchrotron emission from electrons corresponding to this *quasi-thermal* distribution has been computed by Dulk *et al.* (1978) and both X-ray and radio observations are satisfactorally explained if the emitting region is dense (*ca.* 10^{10} electrons cm^{-3}), hot (a few

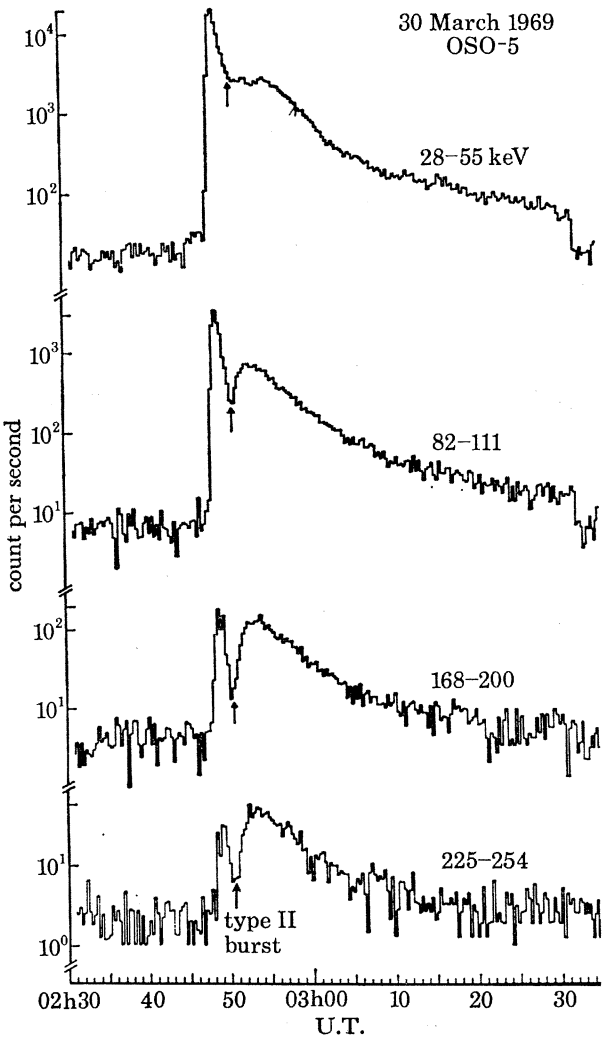

FIGURE 1. An X-ray burst which clearly exhibits the presence of the first and second phases of acceleration. Each intensity–time profile covers the energy interval indicated to the right. Vertical arrows indicate the time of appearance of a type II burst in the metric band. (From Frost & Dennis (1971).)

hundred megakelvins) and compact (characteristic length less than 10^4 km) with a magnetic field strength of a few hundred gauss. It must be noted that, as opposed to the non-thermal model, the deposition of a substantial fraction of the flare energy into the solar atmosphere is not required. Indeed, in the non-thermal model, the non-radiative collisional losses (fast electrons – ambient electron collisions) are much more important than the Bremsstrahlung emission (Ramaty *et al.* 1978). Nevertheless, the main limitation in the 'quasi-thermal' model is that the source must expand.

Two recent observational results seem to prove that this model is reliable: first, the analysis of OSO 5 hard X-ray data has revealed a symmetric rise and fall of the hard X-ray burst (Crannel *et al.* 1978). According to the authors, the existence of this symmetry strongly suggests that the burst is due to a mechanism that is reversible. They proposed that the mechanism is a heating by an adiabatic compression followed by an expansion and a cooling.

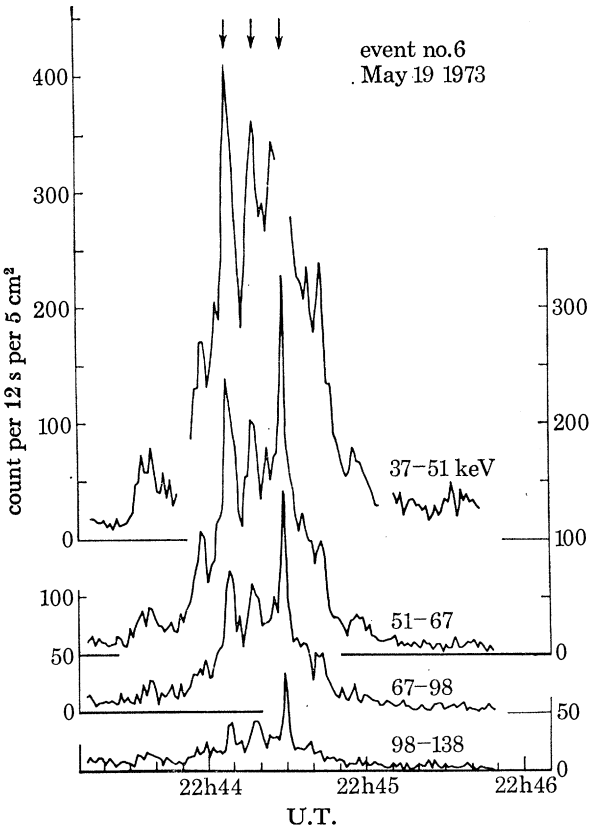

FIGURE 2. An X-ray burst observed with the Utrecht solar hard X-ray spectrometer on board the ESRO TD-1A satellite. The X-ray emission consists of a series of spikes with a duration of a few seconds each. (From Hoyng *et al.* (1976).)

TABLE 1. FIRST PHASE OF ACCELERATION: IMPULSIVE PHASE

	X-ray burst
total duration: less than 1 min: one or several peaks of a few seconds	electron energy: 10–100 keV
non-thermal model: bremsstrahlung on thick cold target $n_i \geqslant 10^{12}$ cm^{-3} energy distribution: *tail*	10^{34}–10^{37} electrons s^{-1}, power law distribution, $E_0 > 25$ keV; $\gamma = 3$–5
	energy deposition: 10^{27}–10^{29} erg s^{-1}†
'*quasi thermal*' *model:* Maxwellian energy distribution $T_e \geqslant 10^8$ K $n_e \simeq 10^{10}$ cm^{-3}	energy deposition: 10^{21}–10^{23} erg s^{-1}
	radio burst
thermal or quasi-thermal model: gyrosynchrotron emission $B \geqslant 100$ G (10^{-2} T)	10^{33}–10^{37} electrons (total) above 10 keV (mostly above 100 keV)

† 1 erg = 10^{-7} J.

On the other hand, centimetric high spatial resolution observations obtained with the Westerbork instrument also suggest similar behaviour. As the intensity increases, the burst source contracts, reaching a minimum size close to the maximum. This is followed by an increase of the burst size after the maximum, indicating possibly an extension. The size at the moment where the maximum intensity is reached ranges between 7″ and 23″ (Alissandrakis *et al.* 1978).

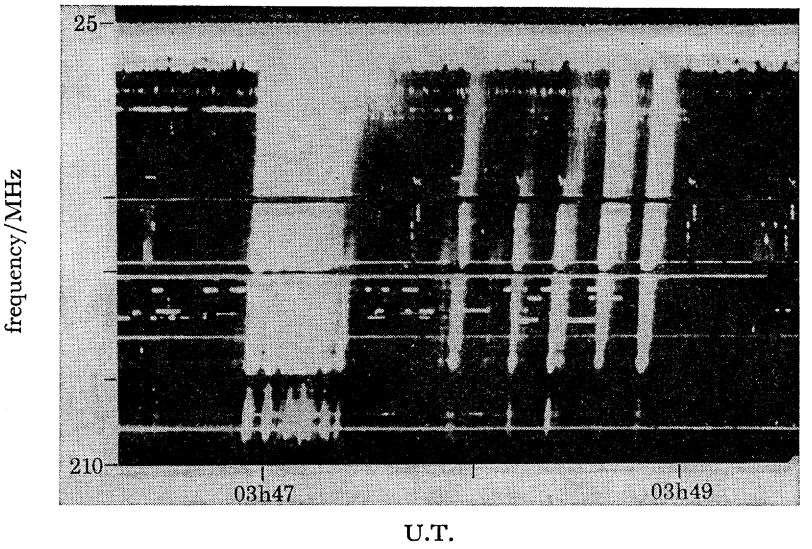

FIGURE 3. Type III bursts in which quasi-periodic spacing is evident. In the first part the spacing is about 5 s, in the latter about 10 s. (From Wild (1963).)

TYPE III RADIOBURSTS

Type III bursts are easily identified on a radio spectrum where they are characterized by a rapid frequency drift from high to low frequencies and by a short duration (figure 3). The bursts cover a very broad frequency range since they are observed at frequencies as high as several hundred megahertz to as low as 10 kHz. They are often produced in coincidence with one spike of the impulsive burst and it is now well accepted that the generation of type III bursts is due to energetic electrons of a few tens of kiloelectronvolts streaming outward through the corona. These electrons excite electron plasma oscillations at each level in the solar atmosphere which are converted through nonlinear processes into electromagnetic waves at the local plasma frequency f_p or/and its first harmonic at $2f_p$. The decreasing frequency with increasing time is attributed to the decreasing electron density and hence the plasma frequency, as the electrons move out of the corona. The lowest frequencies are produced in the interplanetary medium.

Although the detailed mechanism of the electromagnetic waves is not yet clearly understood, the reliability of the plasma hypothesis is largely proved. In particular, *in situ* measurements were provided by space experiments and both electron events and electron plasma oscillations associated with type III bursts have been now detected in the interplanetary medium. Whereas the association between electron events and type III bursts was clearly established in 1972 by Alvarez *et al.*, plasma oscillations were not detected by Earth orbiting satellites. The first observations of electron plasma oscillations with an amplitude sufficient to explain type III bursts were obtained with the German–American Helios 1 and Helios 2 spacecrafts, orbiting around the Sun at a distance between 0.29 and 1.00 AU (Gurnett & Anderson 1976; Gurnett

et al. 1978*b*), then later on, with the Voyager 1 and 2 spacecrafts. Electron plasma oscillations correspond to a succession of narrow band spikes plausibly close to the local plasma frequency. Only 12% of the type III bursts that were observed at frequencies below 178 kHz were produced in association with detectable plasma oscillations, but it was found that both the intensity and the probability of occurrence of plasma oscillation events increase with a decreasing radial distance from the Sun. Close to the Sun, at distances smaller than 0.5 AU, the intensity of these oscillations can reach 1–10 mV m^{-1}, which is in agreement with the field strength required by the theory.

Stereoscopic direction-finding measurements from 2 or 3 different spacecraft were used to determine the three-dimensional positions in the interplanetary medium of type III bursts at several frequencies (Gurnett *et al.* 1978*a*). The interest of this method is that the positions are determined without any assumption of the electron density model. By comparing, in one case, the location of the observed emission frequencies of the type III burst with the measured local electron plasma frequencies, it was directly shown that the type III radio emission occurs close to the second harmonic $2f_p$. This confirms previous results (cf. Fainberg *et al.* 1972).

In summary, the great interest of type III burst observations at very low frequencies is, first, to check the emitting mechanism by comparison between the radio observations and the *in situ* measurements, and secondly, to map the heliosphere by localization of the type III burst sources at several frequencies. One must note that low frequency type III bursts have a long duration, more than 30 min at 100 kHz. All the details are smoothed and in particular the successive events from a same group are often not distinguishable. That is not so at much higher frequencies, when the type III bursts are produced in the corona and closer to the particle accelerating source.

TABLE 2. TYPE III BURSTS

mechanisms

electron streams → electron plasma oscillations + conversion into electromagnetic waves (f_p; $2f_p$)

electron energy

10^{32} electrons per burst 10–100 keV gap in the energy distribution

metre–decametre observations

temporal repetition time scale: seconds. Duration 1 s → accelerating mechanism: $\ll$ 1 s
bursts of a same group: globally similar → region of acceleration and injection well defined
quasi-simultaneous multibeams production (along different paths)
1 beam: 2′ at 0.5 sr

WHAT CAN BE LEARNT FROM CORONAL TYPE III BURST OBSERVATIONS: ACCELERATING MECHANISM; ELECTRON BEAM†

(1) First, type III bursts often occur with a quasi-periodic repetition on a time scale of a few seconds or less at metre wavelengths. Each event of a group has a typical duration of 1 s or less (figure 3). The accelerating mechanism must explain the repetitive production of electron beams on this short time scale. The number of electrons required to explain the radiation of one type III burst is roughly 10^{32}–10^{33}.

(2) On the other hand, the typical observed dimensions of metric type III burst sources are a few arc minutes. It was often suggested that the source dimensions are largely affected by

† See table 2.

propagating effects such as coronal scattering on small-scale inhomogeneities and are thus unable to provide any information on the electron beam structure. In fact, if the observations are carried out with a sufficient space and time resolution, recent results obtained with the Nançay Radioheliograph may prove that one can expect to detect the true source of type III

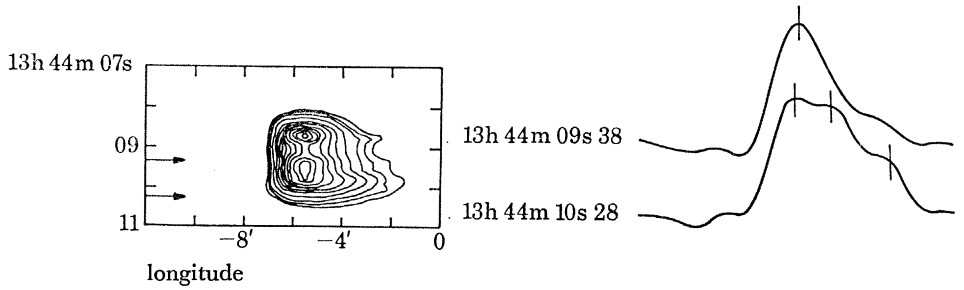

FIGURE 4. Type III bursts observed on 28 December 1977 at 169 MHz with the Nançay Radioheliograph. Left: equal intensity contours are plotted as function of east–west position and time. Horizontal axis, minutes of arc; vertical axis, Universal Time. Right: east–west profiles at a given time, on the same spatial scale. (From Raoult & Pick (1979).)

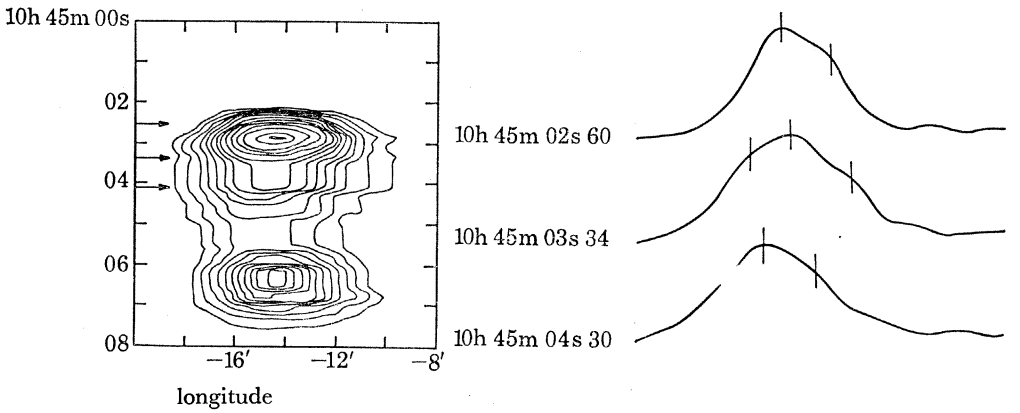

FIGURE 5. Type III bursts observed on 11 September 1977 at 169 MHz with the Nançay Radioheliograph. Left: equal intensity contours are plotted as function of east–west position and time. Horizontal axis, minutes of arc; vertical axis, Universal Time. Right: east–west profiles at a given time, on the same spatial scale. (From Raoult & Pick (1979).)

bursts (Raoult & Pick 1980). The spatial resolution of the Nançay Radioheliograph is 1′ 15″ in the east–west direction and the type III bursts were observed with a time resolution of 0.02 or 0.04 s. These observations reveal that most of the type III burst sources present a complex structure with the presence of multiple components which occur very close in time and often simultaneously (figures 4 and 5). The separation between the different components of a complex burst is most often not greater than 2′. At longitudes smaller than 16′, the sources that are simple always correspond to a diameter smaller than 3′. These observations seem to prove that the sources of type III bursts are in most cases formed with two or more components having a typical size smaller than 3′. Finally, one consequence of the absence of north–south resolution of the instrument is that many sources, though multiple, can appear as single on the disk. Hence, the smallest dimension (2′) that has been observed is probably more representative of the intrinsic size.

In conclusion, the occurrence of type III bursts more often corresponds to the quasi-simultaneous production of two or more electron beams travelling along distinct magnetic paths (Raoult & Pick 1980). These paths can be occasionally highly diverging as reported in one case by Mercier (1975).

(3) Finally, the characteristics of the (size, structure and positions) successive bursts of the same group are in general globally similar over a time period of many seconds (Raoult & Pick 1980). A similar conclusion was drawn for the directivity measured at 169 MHz by stereoscopic observations (Steinberg *et al.* 1974). It may be deduced that the region of acceleration is probably well defined and must not be affected within a time scale of 1 min by the production of the successive electron beams. This region is most often located outside the general bipolar pattern of the active region (Axisa 1974).

References (Pick)

Alissandrakis, C. E. & Kundu, M. R. 1978 *Astrophys. J.* **222**, 342.
Alvarez, H., Haddock, F. & Lin, R. P. 1972 *Solar Phys.* **26**, 468.
Axisa, F. 1974 *Solar Phys.* **35**, 207.
Crannel, C. J., Frost, K. J., Matzler, C., Ohki, K. & Saba, J. L. 1978 *Astrophys. J.***223**, 620.
Dulk, G. A., Melrose, D. B. & Smerd, S. F. 1978 *Proc. astr. Soc. Aust.* **3**, 243.
Dulk, G. A., Melrose, D. B. & White, S. M. 1978 *Astrophys. J.* **234**, 123.
Fainberg, J. L., Evans, L. G. & Stone, R. G. 1972 *Science, N.Y.* **178**, 743.
Frost, K. J. & Dennis, B. R. 1971 *Astrophys. J.* **165**. 655–659.
Gurnett, D. A. & Anderson, R. R. 1976 *Science, N.Y.* **194**, 1159.
Gurnett, D. A., Baumback, M. M. & Rosenbauer, H. 1978*a* *J. geophys. Res.* A **82**, 616.
Gurnett, D. A., Anderson, R. R., Scarf, F. L. & Kurth, W. S. 1978*b* *J. geophys. Res.* A **83**, 4147.
Hoyng, P., Brown, J. C. & VanBeek, H. F. 1976 *Solar Phys.* **48**, 197.
Kane, S. R. 1974 In *Coronal disturbances* (I.A.U. Symposium no. 57) (ed. G. Newkirk Jr), p. 105.
Kundu, M. R. 1965 *Solar radioastronomy*. New York, London and Sydney: Interscience.
Mercier, C. 1975 *Solar Phys.* **45**, 169–179.
Raoult, A. & Pick, M. 1980 *Astron. Astrophys.* (In the press.)
Ramaty, R., Colgate, S. A., Dulk, G. A., Hoyng, P., Knight, J. W., Lin, R. P., Melrose, D. B., Paizis, C., Orrall, F., Shapiro, P. R., Smith, D. F. & Van Hollebeke, M. 1978 In *Proc. Skylab Workshop on Solar Flares*, ch. 4.
Smith, D. F., Hoyng, P. & Knight, J. 1978 In *Proc. Skylab Workshop on Solar Flares*, ch. 5.
Steinberg, J. L., Caroubalos, C. & Bougeret, J. L. 1974 *Astron. Astrophys.* **37**, 109.
Wild, J. P. 1963 In *The solar corona* (ed. J. W. Evans), p. 115. New York and London: Academic Press.

PHILOSOPHICAL TRANSACTIONS OF THE ROYAL SOCIETY A MATHEMATICAL, PHYSICAL & ENGINEERING SCIENCES

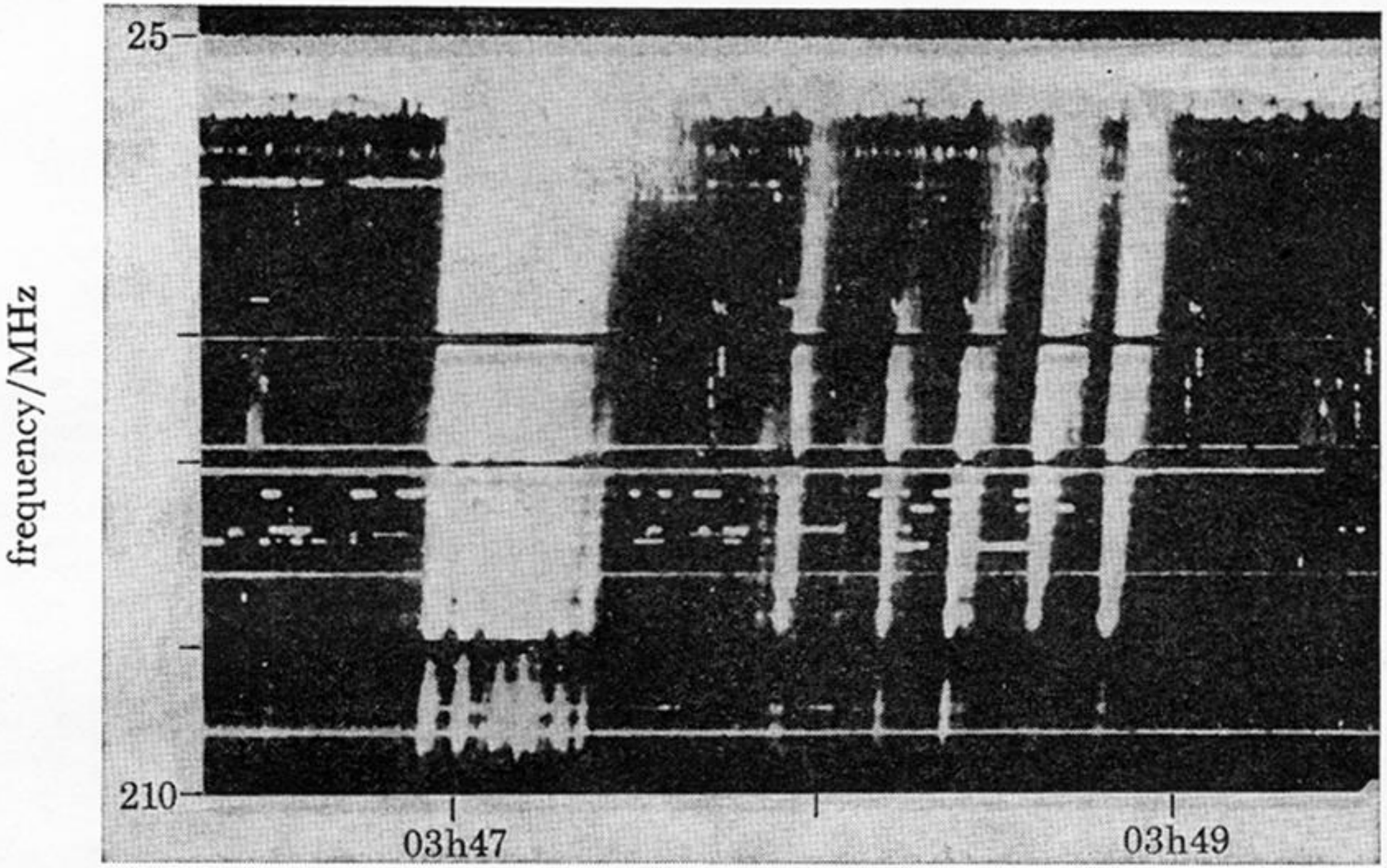

FIGURE 3. Type III bursts in which quasi-periodic spacing is evident. In the first part the spacing is about 5 s, in the latter about 10 s. (From Wild (1963).)

PHILOSOPHICAL TRANSACTIONS OF THE ROYAL SOCIETY A MATHEMATICAL, PHYSICAL & ENGINEERING SCIENCES